Chapter 1

Literature Review

This section reviews various academic sources related to the methodology proposed.

1.1 Introduction

This research project brings together various disciplines of research. By combining techniques from computer vision, sensors and data fusion we can design and develop new way of capturing human gait data.

1.2 Human Motion and Gait

The human gait is well understood and has been studied in detail as it is a fundamental part of human mobility. It is one of the first skills developed in infancy and its importance for healthy develpoment, as outlined by Adolph et al. [1], cannot be understated. Walking and running are also critical factors in transportation and geographical movement of people and goods in developing countries where public transport is underdeveloped and private transport not within the means of the populous. Finally walking and running as exercise has proven benefits as shown in [2] (general health) and [3] (mental health).

There is thus clear evidence that the human gait has earned its right as a field of study in academia.

1.3 Computer Vision

While the previous section answers ”why” understanding the human gait is important, the following sections will explain fields that contribute to the question of ”how” the gait is studied.

Computer vision is a field borne from image processing and artificial intelligence that seeks to replicate the ability of the human visual system.

1.3.1 Computer Vision in robotics

1.3.2 New Perspectives from Animal Borne Cameras

In large this researched project was inspired by work done in the Mechatronics Lab at the University of Cape Town. In 2017, Patel et al. [4] showed that using animal borne cameras and motion sensors, the tail kinematics of the cheetah (Acinonyx Jubatus) could be tracked. Patel's work was partly inspired by Kane et al. [5] where falcon (Falco Peregrinus) borne cameras were used to better understand airborne pursuit of prey.

Further work completed by Pearson et al. [6] showed that cameras mounted to dolphins (Lagenorhynchus obscurus) could provide insight into the their movement, social and foraging strategies. These examples show the promise that animal borne

1.3.3 Human Motion Analysis Using Computer Vision

1.4 Inertial Measurement Units

IMU's are a staple of electrical engineering as applied to dynamic systems. These sensors give us insight as to how an object is moving in space by providing data relating to orientation and acceleration of said system. These data points are created by electronically interpreting signals generated by micro-electromechanical system (MEMS). Modern smartphones have built in IMU's that are not only accurate [7], but also easy to interface with due to the open source nature of the Android operating system [8].

Generally IMUs contain the following subsystems:

- Accelerometer
- Gyroscope
- Magnetometer
- Barometer
- Temperature

Accelerometers provide linear acceleration data; these accelerations may be constant (eg. gravity) or changing (eg. relative motion). In smartphones they are usually based on MEMS that use

Gyroscope

Magnetometer

Barometer

Temperature

1.4.1 Inertial Measurement Units in robotics

1.4.2 Human Motion Analysis Using Inertial Measurement Units

1.5 Mathematical Modelling

The binding element presented in this work is the underlying mathematics

1.5.1 math model of the human gait

1.5.2 linear kinematics

1.5.3 rotational matrices

1.5.4 KF and EKF

The Kalman filter is a mathematical used to estimate

1.6 Observing Natural Solutions for Robotic Shortcomings

Naturally the question arises: why would we want to better understand the dynamics of animals? A persistent problem in the field of modern robotics is that of mobility; robots struggle to navigate real world surfaces and obstacles. Work by Patel et al. [9] shows how we can look towards nature for inspiration to solve this mobility problem.

This follows the central philosophy of bio-inspired robotics as defined by

As demonstrated by various prototype robots built by Boston Dynamics bipedal robots are severely limited in manoeuvrability when compared to

1.7 conclusion

Chapter 2

Methodology

To ensure the success of this project a basic plan of action was created. The following diagram shows the critical phases of the project.

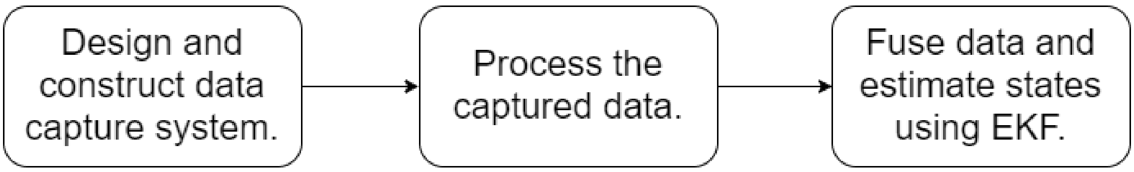

Figure 2.1: Diagram showing the progression and dependence of the major stages of this project

Due to the availability of equipment, financial limitations and time

2.1 System Design

This section is dedicated to defining and understanding the specifications of the data capture system. The system will consist of 4 cameras and an IMU mounted to the torso of the subject. the cameras will record the legs of the subject while the IMU will log inertial data from the body of the subject.

Due to the availability of equipment provided by the Mechatronics Lab the following equipment was chosen as the main components to use in the system:

Item	Selected Equipment	From
Camera	4 GoPro Hero Session Cameras	[10]
IMU	1 Sony Xperia Z3 Compact	[11]
Chest Mount	1 Action Mount Chest Mount	[12]

Table 2.1: The main components used.

The specifications of this data capture system has been defined as:

- Stereo housing to hold the cameras.
- Chest mount to hold the cameras and IMU.
-
-

2.2 Modelling the Lower Limbs

2.3 Experimental Details

The data was captured during a short

2.4 Limitations

Chapter 3

Designing the Data Capture System

To obtain data for the Extended Kalman Filter, a data-capture system needed to be designed. Since the data sources have been identified as multiple video sources and a 9-DOF IMU.

3.1 Camera Mount Design

3.2 Designing the Body Harness

sdfgsdfgsdfg

adsfasdfsdfg

sdfgsdfgdsf

sdfgdsfgdsfg

3.3 Vision Calibration

matlab stereo camera calibration software 1. calibrate the cameras 2. get data from the recordings

took some vids

made matlab script to isolate frames in vids

put frames into stereo video camera calibrator

winning at life

Figure 3.1: GoPro Chesty camera mount from [13]

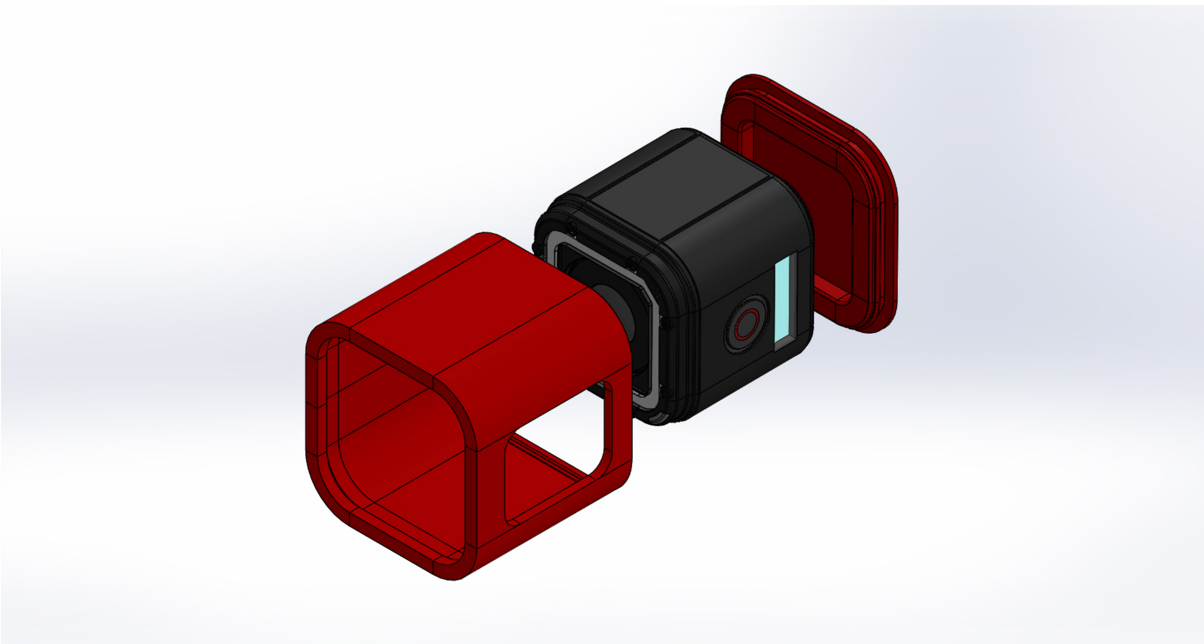

Figure 3.2: Solidworks model of the GoPros Hero 4 Session

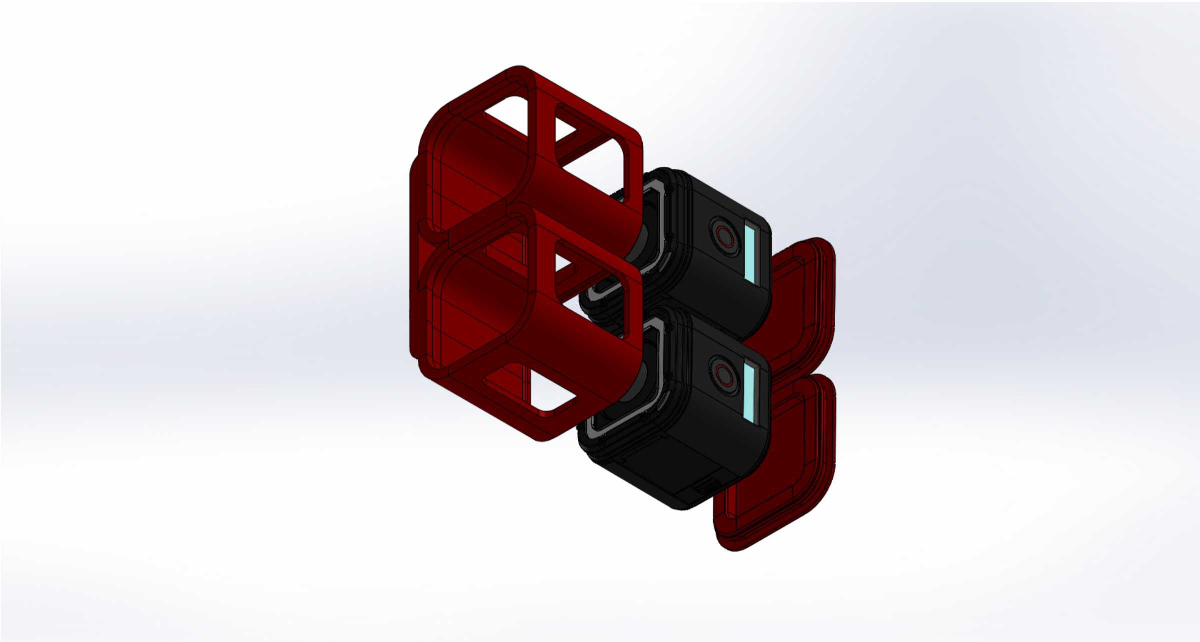

Figure 3.3: angle 1

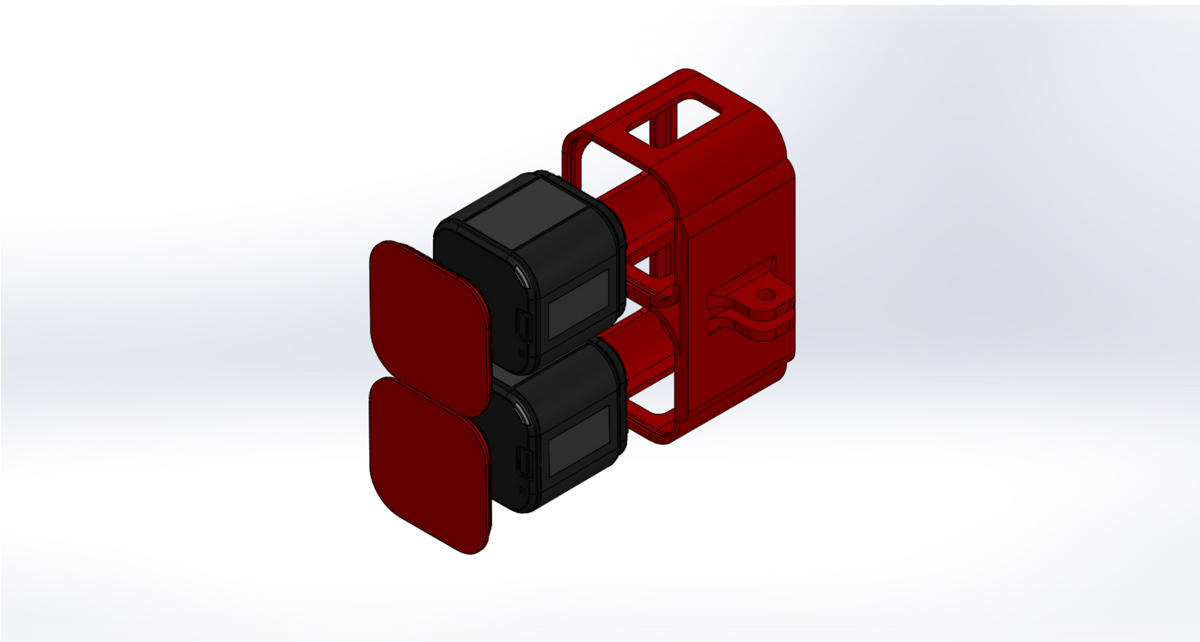

Figure 3.4: angle 2

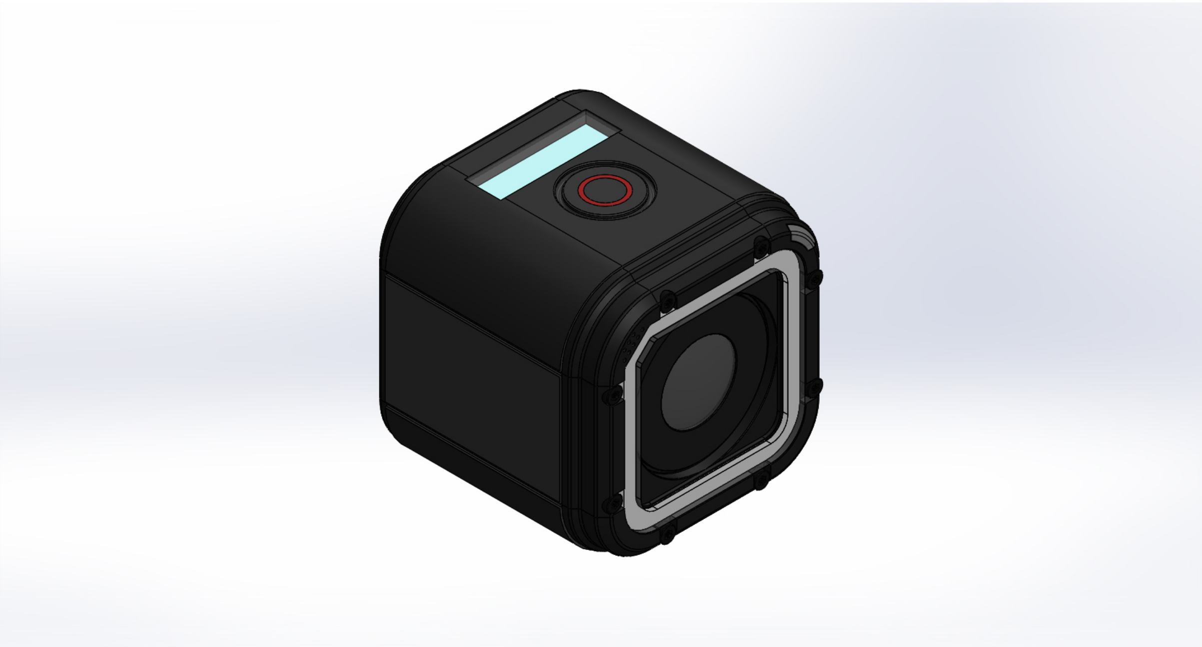

Figure 3.5: Solidworks model of the GPHS Action Camera from [14]

Chapter 4

Processing the Captured Data

This chapter is dedicated to the complex process of extracting critical data from the video files. The following digram shows the process of converting a data heavy video file to a more lightweight .csv (Comma Separated Values) file.

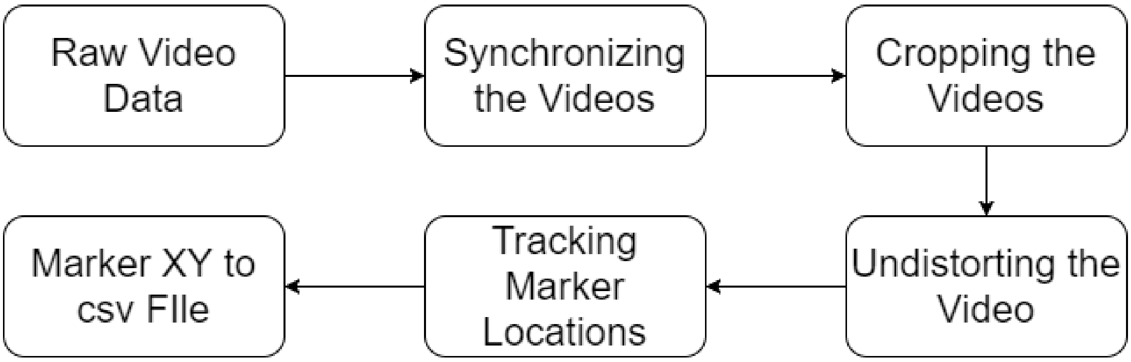

Figure 4.1: Diagram showing the progression and dependence of the major stages of video processing in the project

4.1 Obtaining Video Data

Using the chest mounted cameras detailed in the previous chapter we can generate raw video data. The GPHS cameras can be configured to record at different frame rates and resolutions.

4.2 Synchronizing Video Sources

I typical problem faced when working with different sources of data is that of synchronization. Since this project used 4 different cameras, synchronizing the video sources are critical to generate accurate stereo vision data.

The problem of synchronization was overcome by using a audio cue to align the video data post capturing. With all systems recording, a simple hand clap can serve as a spiking audio input easily identified in the audio track of the video streams. The frame associated with this audio spike can be identified using SVP (Sony Vegas Pro) video editing software as shown in the figure below.

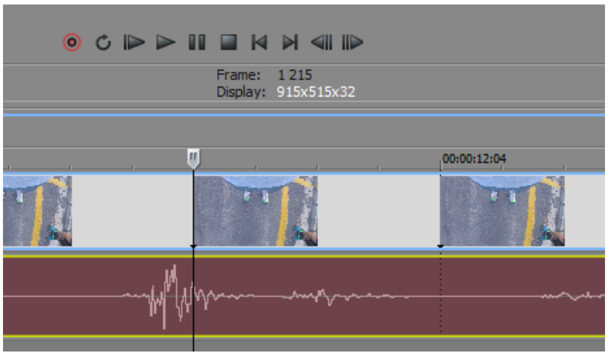

Figure 4.2: Figure showing the user interface of SVP video editing software

The red track in the above figure shows the recorded audio stream while the corresponding frames are displayed in the blue track above that. The cursor is aligned with the audio spike caused by the clap with the corresponding frame number displayed below the playback controls.

This method was repeated for every video stream such that a common starting point was generated.

4.3 Cutting Critical Video Data

With the video data synchronized the next step was to generate a subset of video demonstrating a transient period and steady state period of running. From accelerometer readings we can easily determine the gait cycle period of our subject; that is the amount of time take between the same foot impacting the ground. These impacts are visible as spikes as seen in the accelerometer data.

4.4 Undistorting the Video Data

To generate accurate distances using stereo vision the video frames need to be undistorted.

Distortion of the frames is a result of the

[?]

4.5 Tracking and Exporting Marker Positions in the Frame

using work from [15]

Chapter 5

Data Fusion and State Estimation

This chapter is dedicated the explaining the mathematical methods and models used to fuse data generated by the cameras and IMU.

State	Description
x_{body}	x Position of body w.r.t. the global frame
y_{body}	y Position of body w.r.t. the global frame
z_{body}	z Position of body w.r.t. the global frame
θ_{body}	Pitch of body w.r.t. the global frame
ϕ_{body}	Roll of body w.r.t. the global frame
ψ_{body}	Yaw of body w.r.t. the global frame
θ_{LH}	Pitch of left thigh w.r.t. left hip
ψ_{LH}	Yaw of left thigh w.r.t. left hip
θ_{LK}	Pitch of left calf w.r.t. left knee
θ_{LA}	Pitch of left foot w.r.t. left ankle
θ_{RH}	Pitch of right thigh w.r.t. right hip
ψ_{RH}	Yaw of right thigh w.r.t. right hip
θ_{RK}	Pitch of the right calf w.r.t. right knee
θ_{RA}	Pitch of the right foot w.r.t. the right ankle

Table 5.1: Table showing the different states of the model to be determined by the kalman filter.

we will use derivatives

al the derivatives

$$q = [x_{body}\ y_{body}\ z_{body}\ \theta_{body}\ \phi_{body}\ \psi_{body}\ \theta_{LH}\ \psi_{LH}\ \theta_{LK}\ \theta_{LA}\ \theta_{RH}\ \psi_{RH}\ \theta_{RK}\ \theta_{RA}]$$

all the states totalling 42 states

$$Q = [q\ \dot{q}\ \ddot{q}]$$

all 42 and their equations

positional

$$\ddot{x}_{k+1} = \ddot{x}_k + \sigma^2_{\ddot{x}}$$
$$\dot{x}_{k+1} = \dot{x}_k + \ddot{x}_k T + \sigma^2_{\dot{x}}$$
$$x_{k+1} = x_k + \dot{x}_k T + \sigma^2_x$$

angular

$$\ddot{\theta}_{k+1} = \ddot{\theta}_k + \sigma^2_{\ddot{\theta}}$$
$$\dot{\theta}_{k+1} = \dot{\theta}_k + \ddot{\theta}_k T + \sigma^2_{\dot{\theta}}$$
$$\theta_{k+1} = \theta_k + \dot{\theta}_k T + \sigma^2_{\theta}$$

since all states are either positional(body) or angular(body and limbs) matrices: rotational matrices

$$\text{x axis} \begin{bmatrix} 1 & 0 & 0 \\ 0 & \cos\phi & -\sin\phi \\ 0 & \sin\phi & \cos\phi \end{bmatrix}$$

$$\text{y axis} \begin{bmatrix} \cos\theta & 0 & \sin\theta \\ 0 & 1 & 0 \\ -\sin\theta & 0 & \cos\theta \end{bmatrix}$$

$$\text{z axis} \begin{bmatrix} \cos\psi & -\sin\psi & 0 \\ \sin\psi & \cos\psi & 0 \\ 0 & 0 & 1 \end{bmatrix}$$

solving for the angles

front cameras
point 1 right knee
point 2 left knee
point 3 right foot
point 4 left foot

back cameras
point 1 right calf
point 2 left calf
point 3 right heel
point 4 left heel

front
right knee

$$p1xyz = bodyY + bodyZ + R1 * Thigh$$

left knee

$$p2xyz = bodyY + bodyZ + R1 * Thigh$$

right foot

$$p3xyz = bodyY + bodyZ + R1 * Thigh + R2 * Calf + R3 * Foot$$

left foot

$$p4xyz = bodyY + bodyZ + R1 * Thigh + R2 * Calf + R3 * Foot$$

back

right calf

$$p1xyz = bodyY + bodyZ + R1 * Thigh + R2 * 0.5 * Calf$$

left calf

$$p2xyz = bodyY + bodyZ + R1 * Thigh + R2 * 0.5 * Calf$$

right heel

$$p2xyz = bodyY + bodyZ + R1 * Thigh + R2 * Calf$$

left heel

$$p2xyz = bodyY + bodyZ + R1 * Thigh + R2 * Calf$$

Chapter 6

Results, verification and Discussion

Chapter 7

Conclusions and Future Work

Bibliography

[1] K. E. Adolph and S. R. Robinson, "The road to walking: What learning to walk tells us about development," *Oxford handbook of developmental psychology*, vol. 1, pp. 403–443, 2013.

[2] S. Hanson and A. Jones, "Is there evidence that walking groups have health benefits? a systematic review and meta-analysis," *Br J Sports Med*, vol. 49, no. 11, pp. 710–715, 2015.

[3] K. R. Fox, "The influence of physical activity on mental well-being," *Public health nutrition*, vol. 2, no. 3a, pp. 411–418, 1999.

[4] A. Patel, B. Stocks, C. Fisher, F. Nicolls, and E. Boje, "Tracking the cheetah tail using animal-borne cameras, gps, and an imu," *IEEE Sensors Letters*, vol. 1, no. 4, pp. 1–4, 2017.

[5] S. A. Kane and M. Zamani, "Falcons pursue prey using visual motion cues: new perspectives from animal-borne cameras," *Journal of Experimental Biology*, vol. 217, no. 2, pp. 225–234, 2014.

[6] H. C. Pearson, P. W. Jones, M. Srinivasan, D. Lundquist, C. J. Pearson, K. A. Stockin, and G. E. Machovsky-Capuska, "Testing and deployment of c-viss (cetacean-borne video camera and integrated sensor system) on wild dolphins," *Marine Biology*, vol. 164, no. 3, p. 42, 2017.

[7] V. Gikas and H. Perakis, "Rigorous performance evaluation of smartphone gnss/imu sensors for its applications," *Sensors*, vol. 16, no. 8, p. 1240, 2016.

[8] Google, "Sensors overview," https://developer.android.com/guide/topics/sensors/sensors_overview.html, [Online; accessed 11-October-2017].

[9] A. Patel and M. Braae, "Rapid turning at high-speed: Inspirations from the cheetah's tail," in *Intelligent Robots and Systems (IROS), 2013 IEEE/RSJ International Conference on*. IEEE, 2013, pp. 5506–5511.

[10] I. GoPro, "Hero session," https://shop.gopro.com/EMEA/cameras/hero-session/CHDHS-104-master.html, [Online; accessed 10-October-2017].

[11] Sony, "Xperia z3 compact," https://www.sonymobile.com/za/products/phones/xperia-z3-compact/, [Online; accessed 10-October-2017].

[12] A. Mount, "Chest mount," http://action-mount.com/products/chest-mount/, [Online; accessed 10-October-2017].

[13] I. GoPro, "Gopro chesty (chest harness)," https://shop.gopro.com/EMEA/mounts/chesty-chest-harness/GCHM30-001.html, [Online; accessed 6-October-2017].

[14] M. Christensen, "Gopro hero4 session," https://grabcad.com/library/gopro-hero4-session-1, [Online; accessed 6-October-2017].

[15] T. L. Hedrick, "Software techniques for two-and three-dimensional kinematic measurements of biological and biomimetic systems," *Bioinspiration & biomimetics*, vol. 3, no. 3, p. 034001, 2008.